Supplementary Data

DKK1 promotes tumor immune evasion and impedes anti-PD-1 treatment by inducing immunosuppressive macrophages in gastric cancer

Tao Shi[1,2], Yipeng Zhang[1], Yue Wang[1], Xueru Song[1], Hanbing Wang[1], Xiaoyu Zhou[3], Kaijie Liang[1], Yuting Luo[1], Keying Che[1], Xuan Wang[4], Yunfeng Pan[1], Fangcen Liu[5], Ju Yang[1], Qin Liu[1], Lixia Yu[1], Baorui Liu[1,2], Jia Wei[1,2,6,7*]

Supplementary table

Table. S1. Clinicopathological characteristics of GC patients with low (Hscore<60) or high (Hscore≥60) DKK1 expression from Drum Tower Hospital Cohort.

Variable	Low DKK1 expression n=139 (48.94%)	High DKK1 expression n=145 (51.06%)	*p*
Age（years）			
<65	71 (51.08)	70 (48.28)	
≥65	68 (48.92)	75 (51.72)	0.724
Gender			
Male	103 (74.1)	113 (77.93)	
Female	36 (25.9)	32 (22.07)	0.537
Lauren classification			
Intestinal type	40 (28.78)	35 (24.14)	
Diffuse type	54 (38.85)	50 (34.48)	
Mixture	45 (32.37)	60 (41.38)	0.286
AJCC			
IIIa-IIIc	128 (92.09)	133 (91.72)	
IV	11 (7.91)	12 (8.28)	1
T-stage			
T1	16 (11.51)	2 (1.38)	
T2	84 (60.43)	83 (57.24)	
T3	39 (28.06)	60 (41.38)	**< 0.001**
N-stage			
N1	14 (10.07)	15 (10.34)	
N2	36 (25.90)	43 (29.65)	
N3	89 (64.03)	87 (60.01)	0.415
M-stage			
M0	136 (97.84)	144 (99.31)	
M1	3 (2.16)	1 (0.69)	0.585
Vascular invasion			
Negative (-)	32 (23.02)	28 (19.31)	
Positive (+)	107 (76.98)	117 (80.69)	0.535
Neural invasion			
Negative (-)	18 (12.95)	7 (4.83)	
Positive (+)	121 (87.05)	138 (95.17)	**0.027**
Her2			
Negative (-)	67 (48.2)	69 (47.59)	
Positive (+ ~ +++)	72 (51.8)	76 (52.41)	1
VEGFR2			
Negative (-)	17 (12.23)	6 (4.14)	
Positive (+ ~ +++)	122 (87.77)	139 (95.86)	**0.022**
E-cadherin			
Negative (-)	14 (10.07)	13 (8.97)	
Positive (+ ~ +++)	125 (89.93)	132 (91.03)	0.908
PDL1			
CPS<10	87 (62.59)	111 (76.55)	
CPS≥10	52 (37.41)	34 (23.45)	**0.015**
NY-ESO-1			
Negative (-)	123 (88.49)	140 (96.55)	
Positive (+ ~ +++)	16 (11.51)	5 (3.45)	**0.018**

CPS, combined positive score.

Supplementary figures

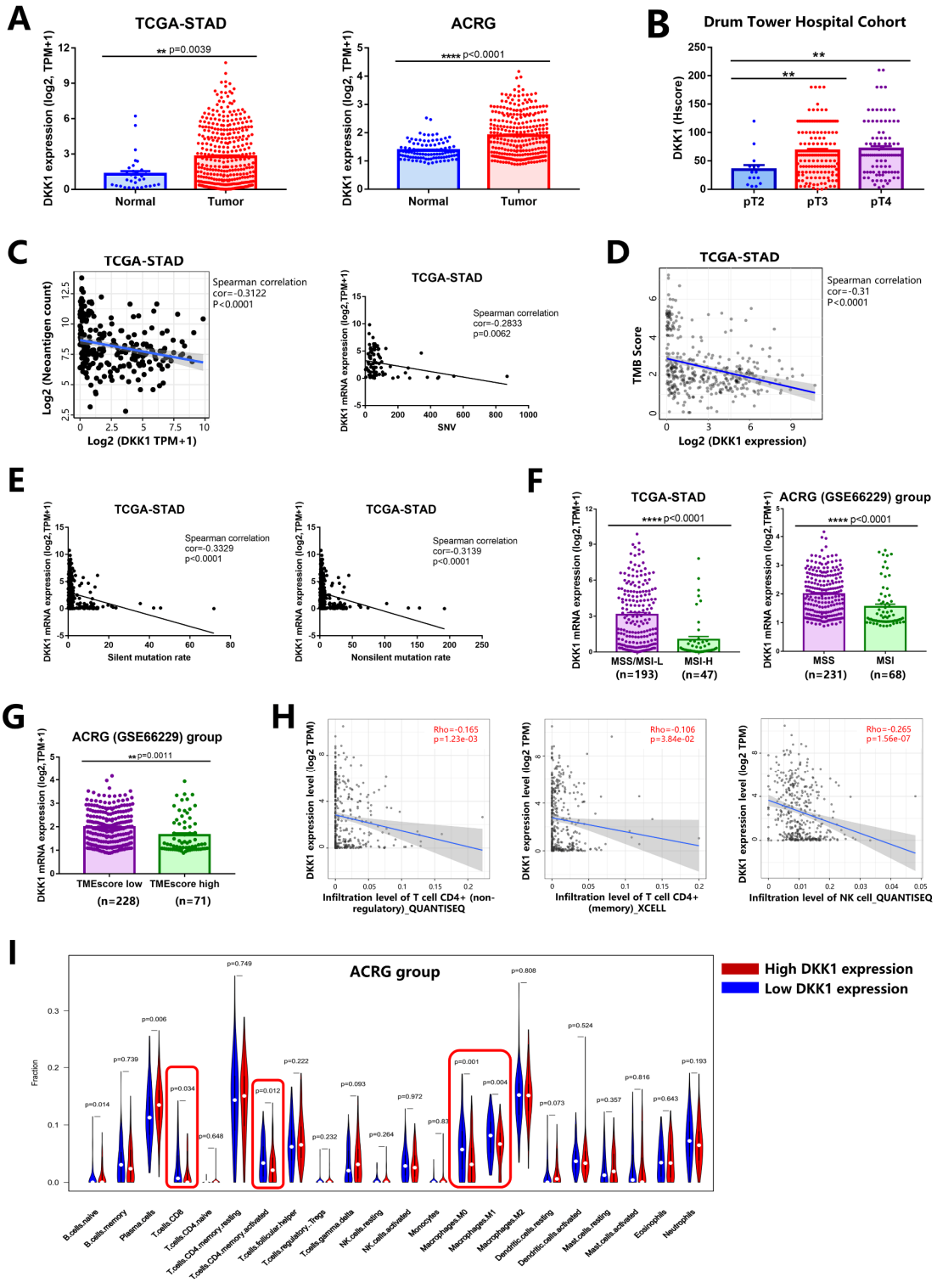

Fig. S1. Supplementary clinical data of DKK1 analysis in GC patients. (A) DKK1 mRNA expression (in TPM) of samples in TCGA-STAD (tumor tissues, n=375; paired normal tissues, n=32) and ACRG group (tumor tissues, n=300; paired normal tissues, n=100). **(B)** DKK1 Hscore of GC

tissues from Drum Tower Hospital Cohort was analyzed in groups with different pathological T stage (pT2, n=15; pT3, n=146; pT4, n=92). **(C)** Predicted neoantigen counts and Single Nucleotide Variants (SNV) were negatively correlated with DKK1 mRNA expression among GC tissues (n=351) from TCGA-STAD. **(D)** Tumor mutation burden (TMB) score was negatively correlated with DKK1 mRNA expression among GC tissues (n=351) from TCGA-STAD. **(E)** Silent and non-silent mutation rates were negatively correlated with DKK1 mRNA expression among GC tissues (n=351) from TCGA-STAD. **(F)** DKK1 mRNA expression of GC tissues with different MSI status from TCGA-STAD (MSS/MSI-L, n=193; MSI-H, n=47) and ACRG (MSS, n=231; MSI, n=68). **(G)** DKK1 mRNA expression of GC tissues from ACRG was analyzed in TME score low (n=228) and high (n=71) groups. **(H)** Tumoral infiltration level of non-regulatory $CD4^+$ T cells, memory $CD4^+$ T cells and NK cells (estimated by QUANTISEQ and XCELL) was negatively correlated with DKK1 mRNA expression among GC tissues (n=375) from TCGA-STAD. **(I)** Intratumoral fractions of 22 immune cells among GC tissues (n=300) from ACRG were estimated by CIBERSORT. Data with error bars are shown as mean ± SEM. ns, not significant; *$P < 0.05$, **$P < 0.01$, ***$P < 0.001$, ****$P < 0.0001$.

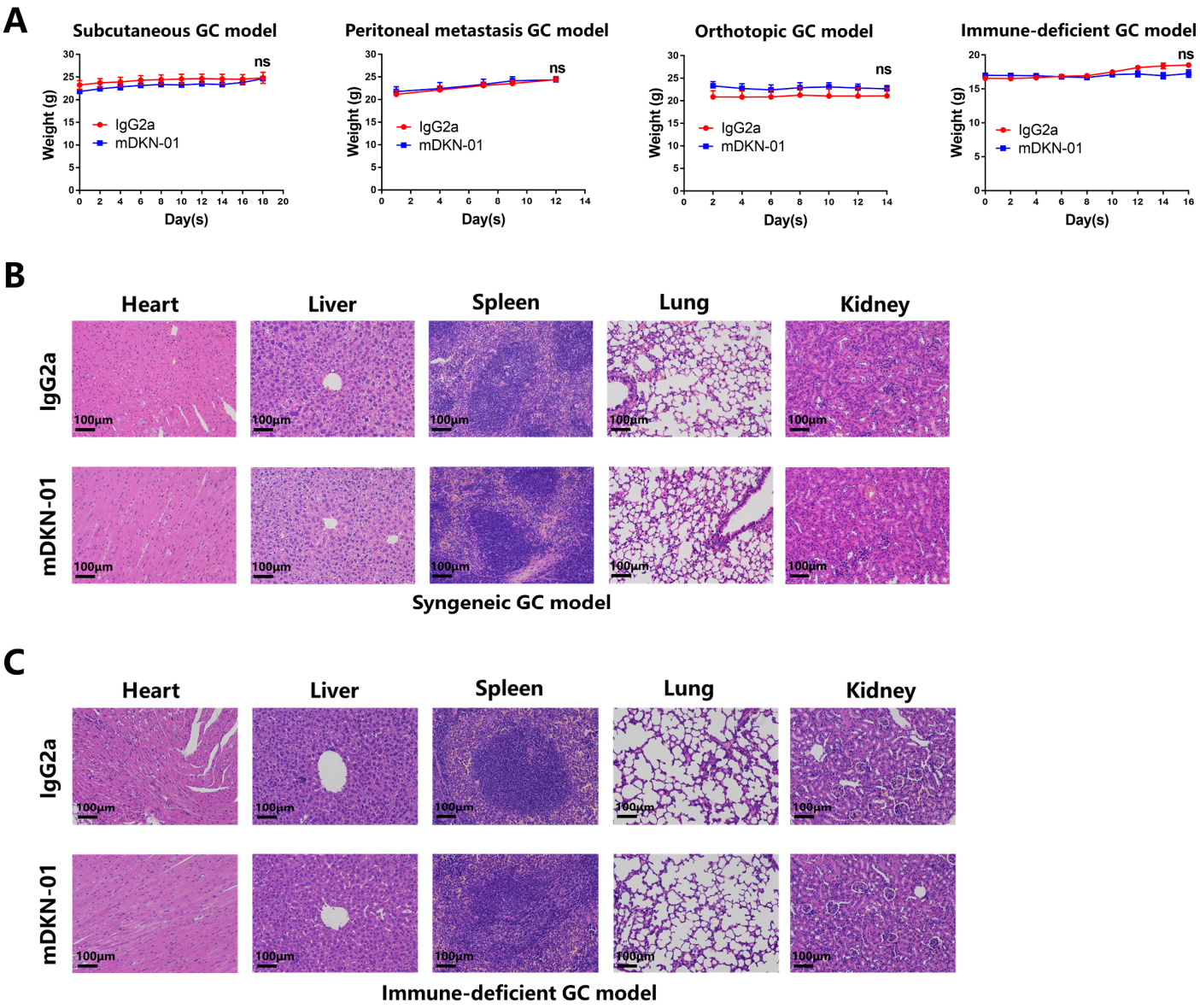

Fig. S2. Safety evaluation of DKK1 blockade in murine GC models. (A) Body weight of mice from different GC models treated with mDKN-01 or IgG2a. **(B-C)** Safety evaluation of mDKN-01 administration in mouse organs from syngeneic or immune-deficient GC model is shown by hematoxylin and eosin (H&E) staining (Scale bars, 100 μm). Data with error bars are shown as mean ± SEM. ns, not significant; **P* < 0.05, ***P* < 0.01, ****P* < 0.001, *****P* < 0.0001.

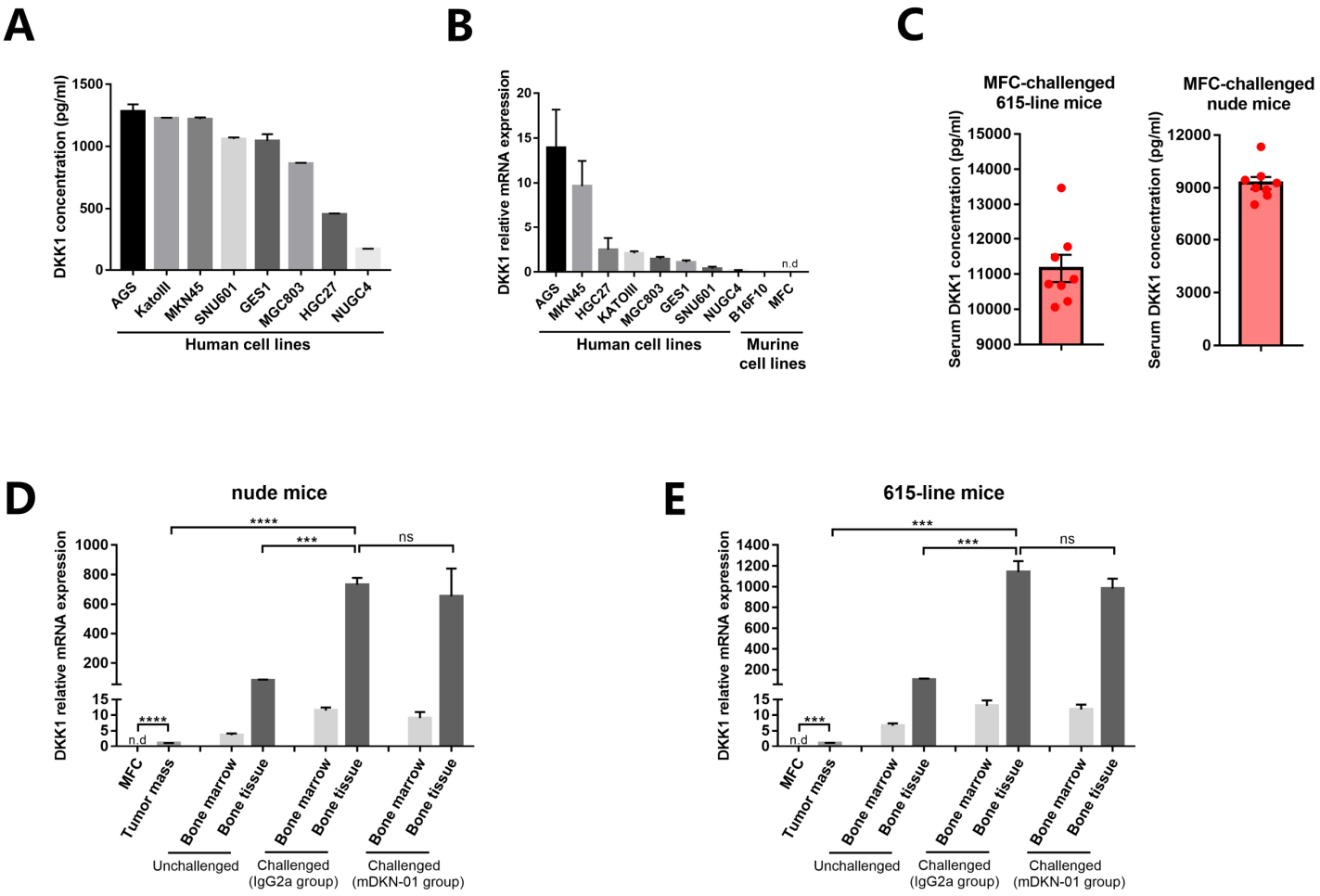

Fig. S3. The source of DKK1 in GC cell lines and mouse GC models. (A) DKK1 protein concentration and **(B)** relative DKK1 mRNA expression and among human and murine cancer cell lines are detected by ELISA and RT-qPCR. Each type of cell line is a representative experiment of at least three independent biological replicates. **(C)** Serum DKK1 concentration of MFC-challenged 615-line and Balb/c nude mice (n=8 per group). **(D)** Relative DKK1 mRNA expression in tumor mass, bone marrow and bone tissue of MFC-challenged 615-line mice (n=3 per group). **(E)** Relative DKK1 mRNA expression in tumor mass, bone marrow and bone tissue of MFC-challenged Balb/c nude mice (n=3 per group). Data with error bars are shown as mean ± SEM. ns, not significant; *P < 0.05, **P < 0.01, ***P < 0.001, ****P < 0.0001.

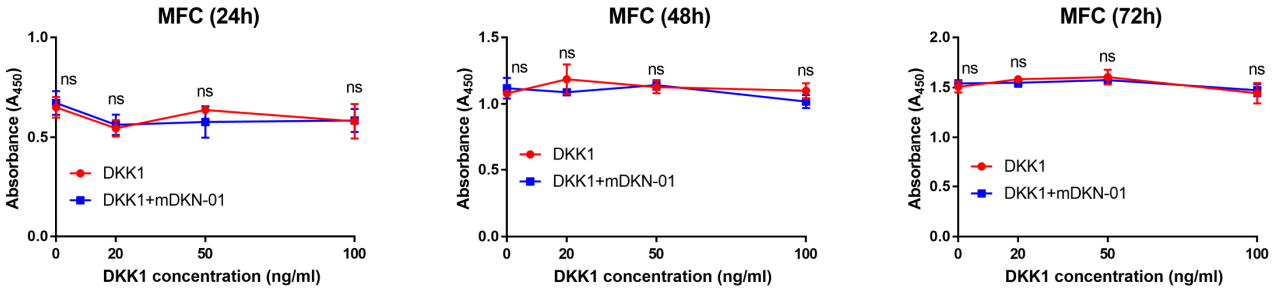

Fig. S4. Effects of DKK1 blockade on MFC cells. MFC cells were seeded in 96-well plates at 4000 cells per well and treated with recombinant DKK1 protein at different concentrations, with or without mDKN-01 at 10 μg/ml. After 24h, 48h or 72h co-culture, cell viability was measured by CCK-8 assay. Data with error bars are shown as mean ± SEM. ns, not significant; **P* < 0.05, ***P* < 0.01, ****P* < 0.001, *****P* < 0.0001.

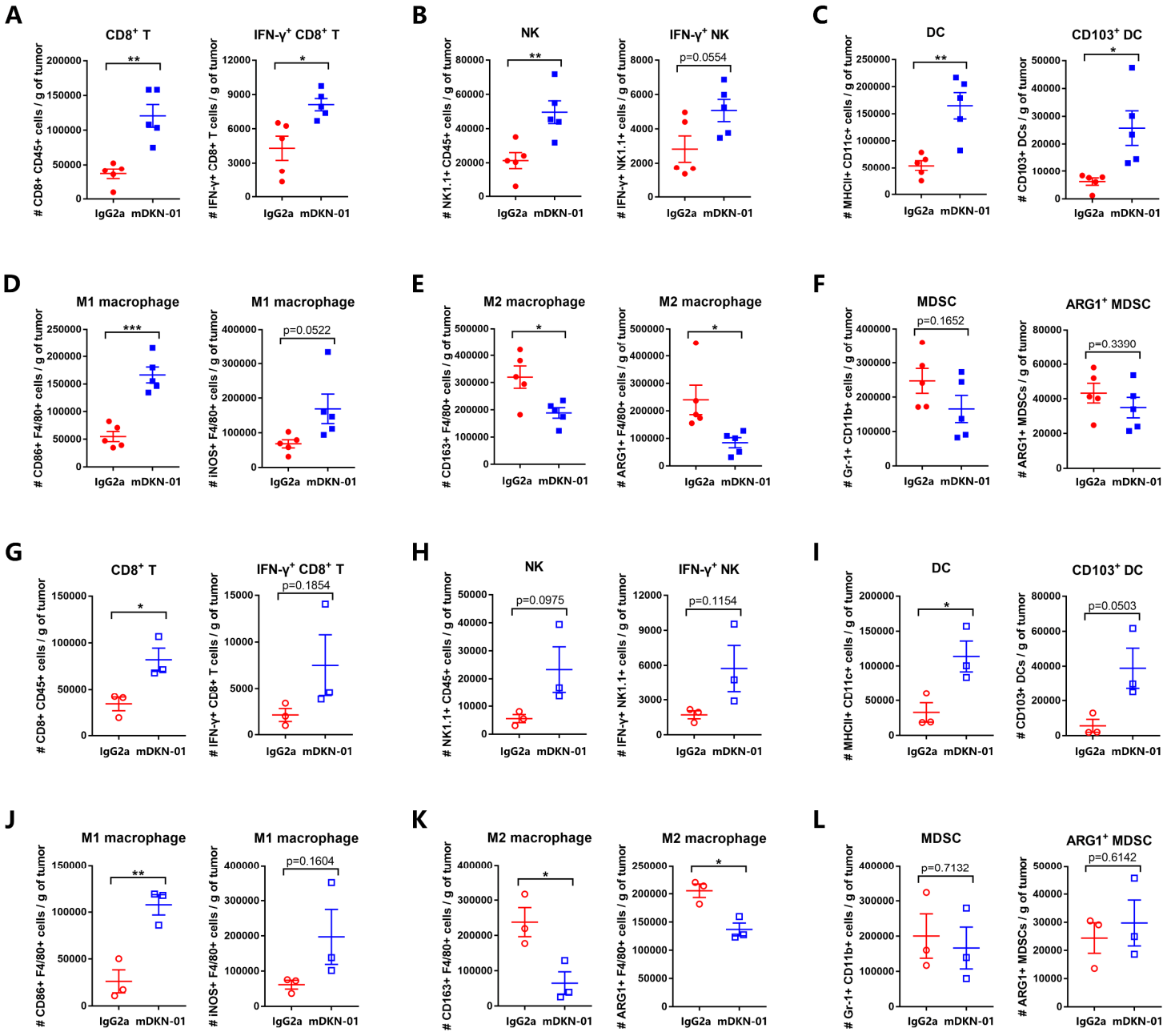

Fig. S5. Absolute counts of immune cells in the TIME of subcutaneous and orthotopic GC model. Absolute counts (normalized to tumor weight) of intratumoral **(A)** $CD8^+$ / $CD45^+$ cells, IFN-γ^+ $CD8^+$ T cells, **(B)** $NK1.1^+$ / $CD45^+$ cells, IFN-γ^+ / $NK1.1^+$ cells, **(C)** MHC-II^+ / $CD11c^+$ cells, $CD103^+$ DCs, **(D)** $CD86^+$ / $F4/80^+$ cells, $iNOS^+$ / $F4/80^+$ cells, **(E)** $CD163^+$ / $F4/80^+$ cells, $ARG1^+$ / $F4/80^+$ cells, **(F)** Gr-1^+ / $CD11b^+$ cells and Arginase 1^+ / $F4/80^+$ cells in subcutaneous GC model were determined by flow cytometry (n=5 per group). Absolute counts (normalized to tumor weight) of intratumoral **(G)** $CD8^+$ / $CD45^+$ cells, IFN-γ^+ $CD8^+$ T cells, **(H)** $NK1.1^+$ / $CD45^+$ cells, IFN-γ^+ / $NK1.1^+$ cells, **(I)** MHC-II^+ / $CD11c^+$ cells, $CD103^+$ DCs, **(J)** $CD86^+$ / $F4/80^+$ cells, $iNOS^+$ / $F4/80^+$

cells, **(K)** CD163^{+} / F4/80^{+} cells, Arginase 1^{+} / F4/80^{+} cells, **(L)** Gr-1^{+} / CD11b^{+} cells and ARG1^{+} / F4/80^{+} cells in orthotopic GC model were determined by flow cytometry (n=3 per group). Data with error bars are shown as mean ± SEM. ns, not significant; *P < 0.05, **P < 0.01, ***P < 0.001, ****P < 0.0001.

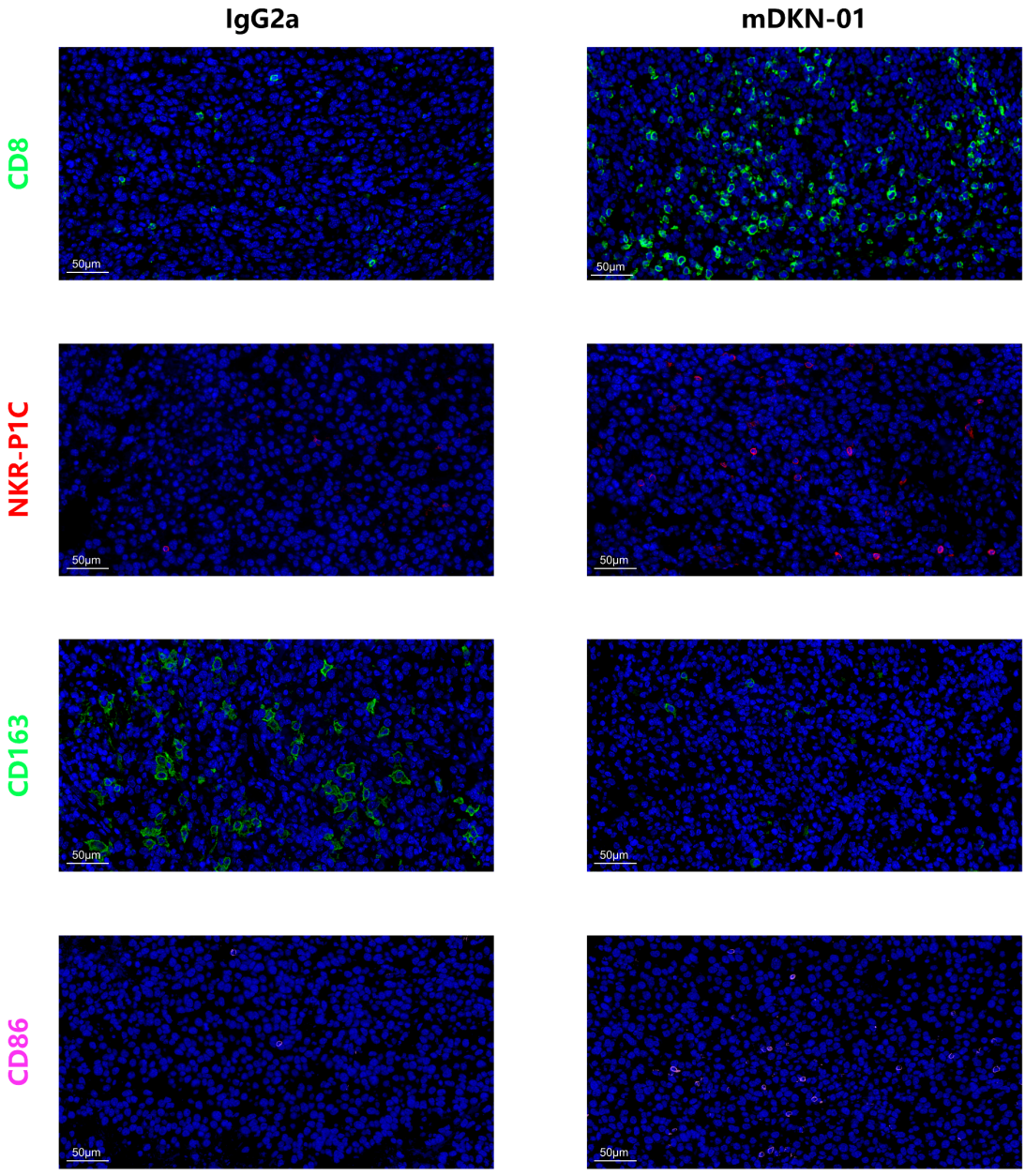

Fig. S6. Immunofluorescence analysis of immune components in the TIME of syngeneic GC model. Representative immunostaining images showing DAPI (blue), CD8 (green), NKR-P1C (red), CD163 (green) and CD86 (pink) in the tumors from the syngeneic GC model (Scale bars, 50 μm).

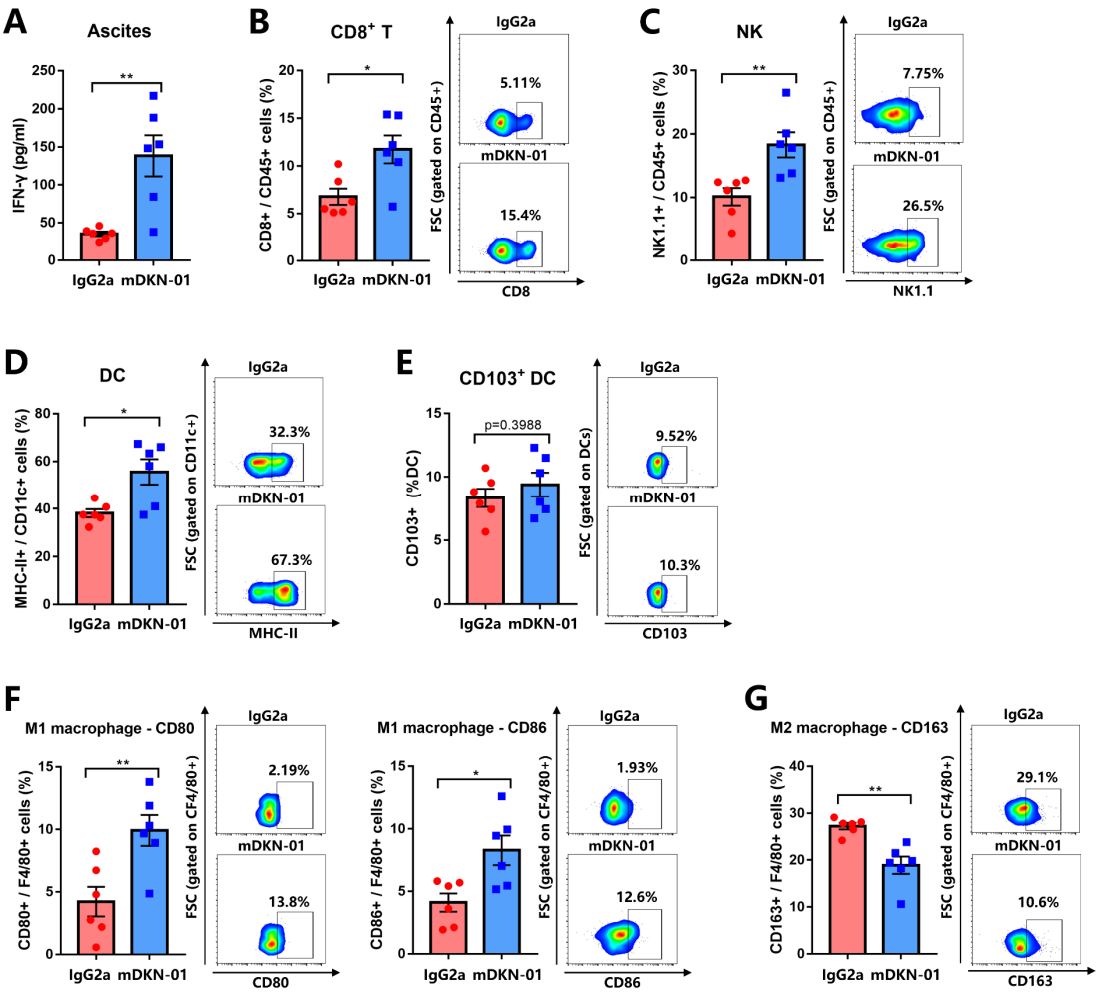

Fig. S7. DKK1 blockade improves infiltration of immune cells in peritoneal metastasis GC model. (A) IFN-γ release in ascites was detected by CBA. The proportions of **(B)** $CD8^+$ / $CD45^+$ cells, **(C)** $NK1.1^+$ / $CD45^+$ cells, **(D)** $MHC\text{-}II^+$ / $CD11c^+$ cells, **(E)** $CD103^+$ DCs, **(F)** $CD80^+$ / $F4/80^+$ cells, $CD86^+$ / $F4/80^+$ cells and **(G)** $CD163^+$ / $F4/80^+$ cells in tumors were determined by flow cytometry. Data with error bars are shown as mean ± SEM. ns, not significant; $*P < 0.05$, $**P < 0.01$, $***P < 0.001$, $****P < 0.0001$.

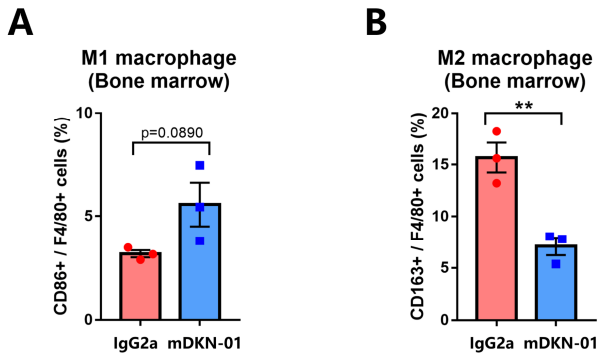

Fig S8. DKK1 blockade improves the M1/M2 ratio of macrophages in the bone marrow of subcutaneous GC model. The proportions of **(A)** $CD86^+$ / $F4/80^+$ cells and **(B)** $CD163^+$ / $F4/80^+$ cells in the bone marrow of MFC-challenged 615-line mice were determined by flow cytometry (n=3 per group). Data with error bars are shown as mean ± SEM. ns, not significant; *P < 0.05, **P < 0.01, ***P < 0.001, ****P < 0.0001.

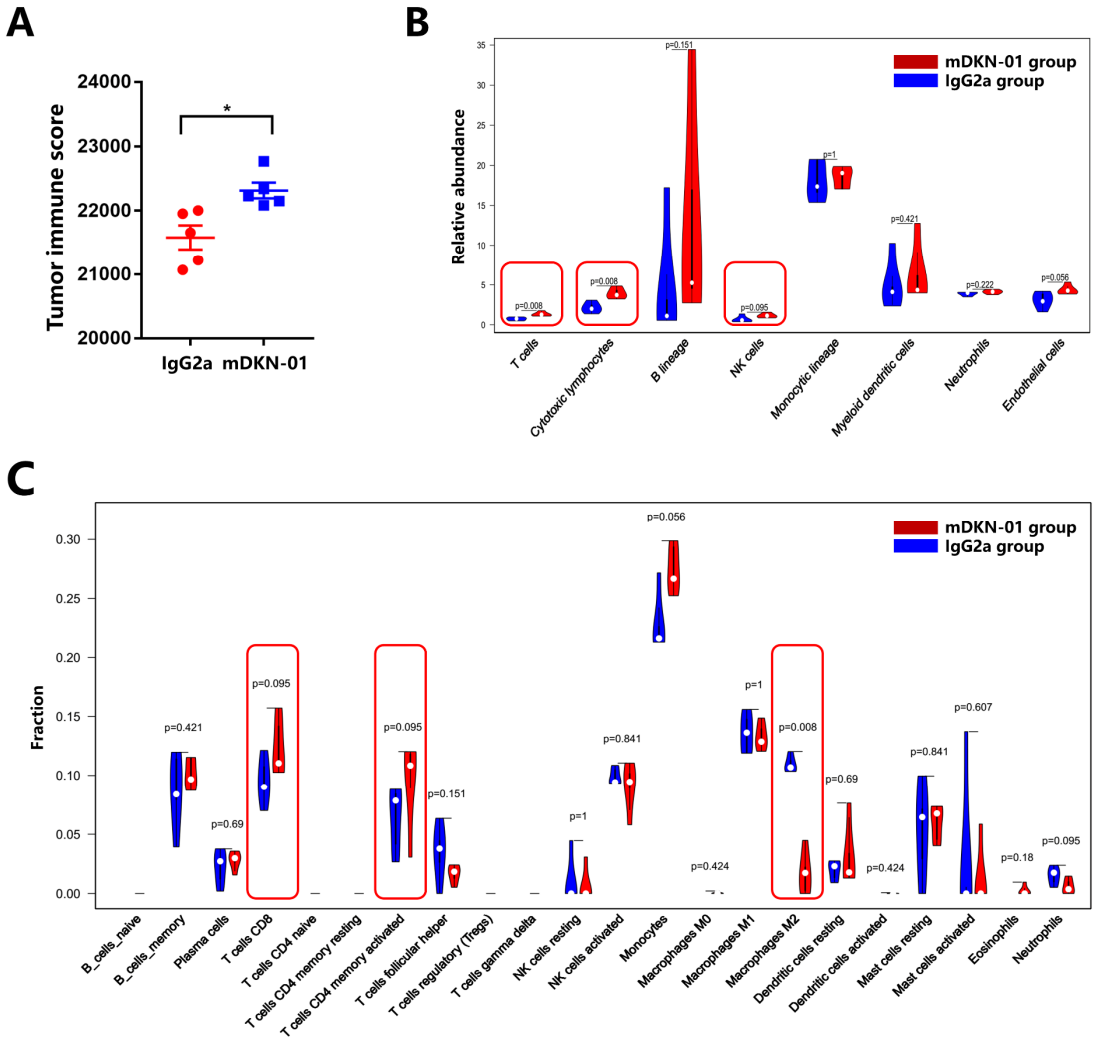

Fig. S9. Supplementary transcriptome sequencing data of tumor tissues derived from syngeneic GC model. MFC-challenged syngeneic GC model was established and treated as described in Fig 2A. Mice were sacrificed at treatment endpoint and tumors were removed for transcriptome sequencing analysis. **(A)** Immune score of tumors was measured by ESTIMATE (n=5 per group). **(B)** Intratumoral fractions of 8 immune cells were estimated by MCP-Counter (n=5 per group). **(C)** Intratumoral fractions of 22 immune cells were estimated by CIBERSORT (n=5 per group). Data with error bars are shown as mean ± SEM. ns, not significant; *$P < 0.05$, **$P < 0.01$, ***$P < 0.001$, ****$P < 0.0001$.

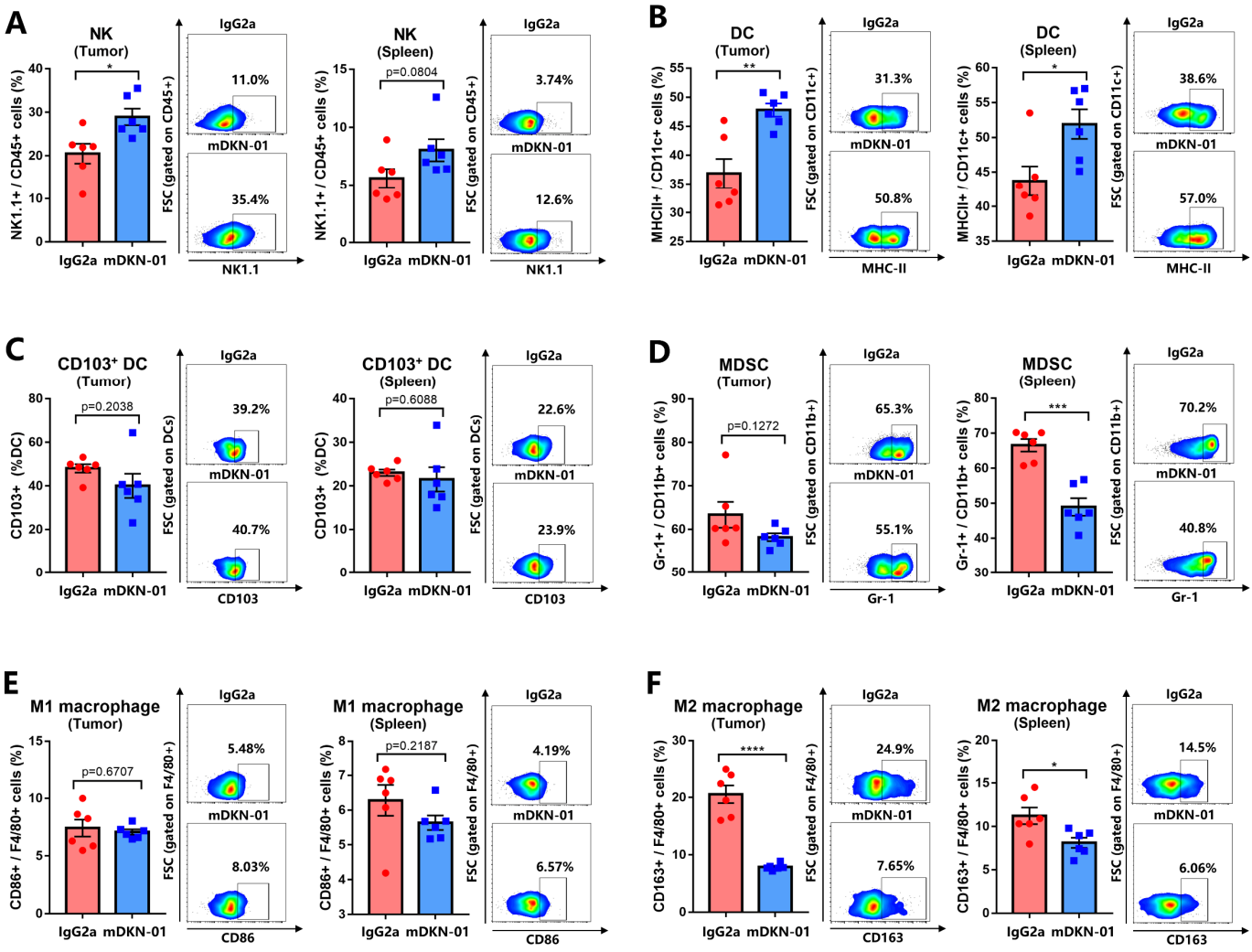

Fig. S10. DKK1 blockade improves innate immunity in T cell-deficient GC model. The proportions of **(A)** NK1.1$^+$ / CD45$^+$ cells, **(B)** MHC-II$^+$ / CD11c$^+$ cells, **(C)** CD103$^+$ DCs, **(D)** Gr-1$^+$ / CD11b$^+$ cells, **(E)** CD86$^+$ / F4/80$^+$ cells and **(F)** CD163$^+$ / F4/80$^+$ cells in tumors and spleens were determined by flow cytometry (n=6 per group). Data with error bars are shown as mean ± SEM. ns, not significant; *P < 0.05, **P < 0.01, ***P < 0.001, ****P < 0.0001.

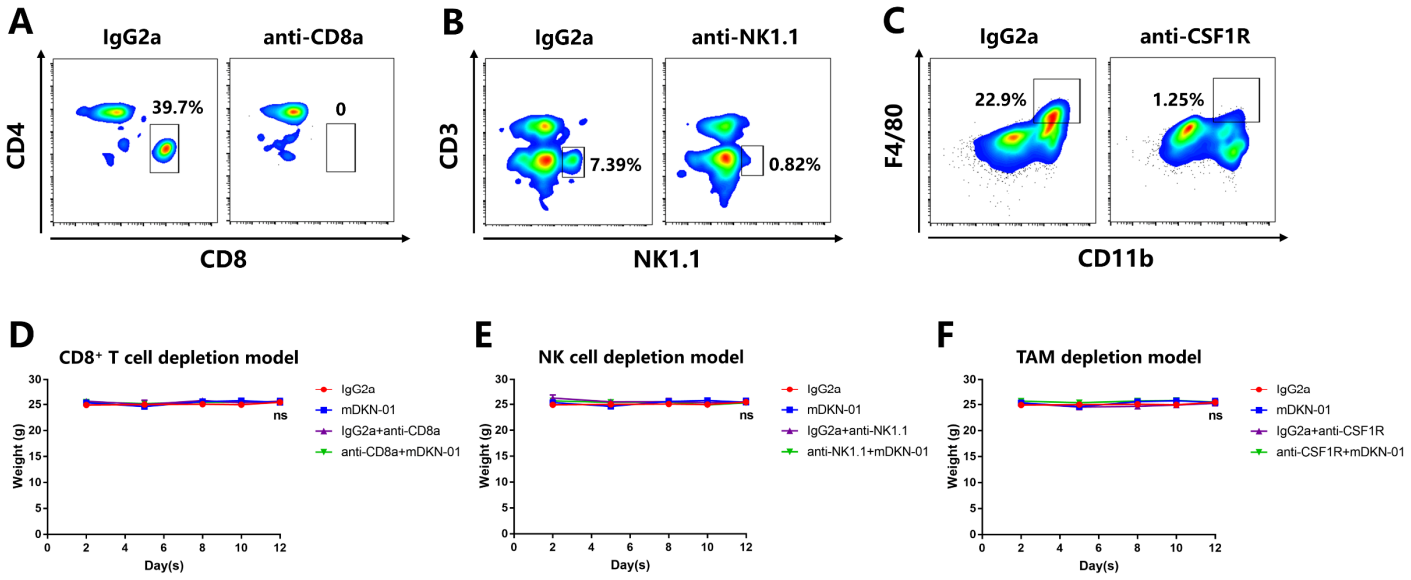

Fig. S11. Immune-depletion check and safety evaluation of DKK1 blockade in different syngeneic GC models. Schematic of the immune cell-depletion and mDKN-01 treatment are as described in Fig 5A, G, M. **(A)** $CD8^+$ T cell and **(B)** NK cell-depletion checked on Day 0. Representative flow charts are shown. **(C)** TAM-depletion checked on Day 14. Representative flow chart is shown. **(D)** Body weight of mice from $CD8^+$ T cell depletion model treated with mDKN-01 or IgG2a (n=6 per group). **(E)** Body weight of mice from NK cell depletion model treated with mDKN-01 or IgG2a (n=6 per group). **(F)** Body weight of mice from TAM depletion model treated with mDKN-01 or IgG2a (n=6 per group). Data with error bars are shown as mean ± SEM. ns, not significant; *$P < 0.05$, **$P < 0.01$, ***$P < 0.001$, ****$P < 0.0001$.

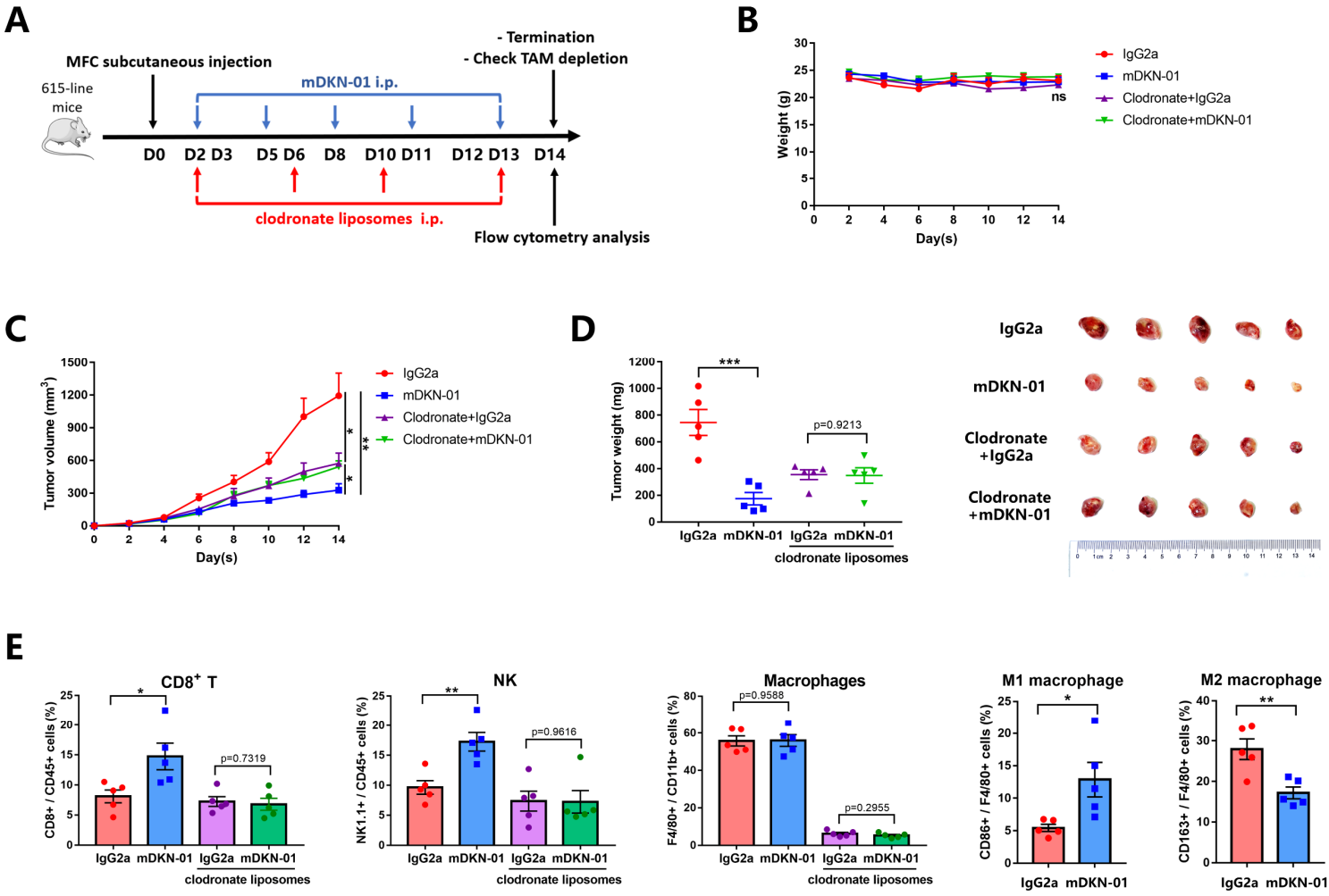

Fig. S12. DKK1 blockade fails to trigger anti-tumor effects or improve the TIME of subcutaneous GC model with TAM-depletion by clodronate liposomes. (A) Schematic of TAM depletion by clodronate liposomes and mDKN-01 treatment in subcutaneous GC model. **(B)** Body weight, **(C)** tumor volume and **(D)** tumor weight of 615-line mice treated with clodronate liposomes, mDKN-01 or IgG2a (n=5 per group). Mice were sacrificed on day 14 and the tumors were removed for analysis. **(E)** The proportions of $CD8^+$ / $CD45^+$ cells, $NK1.1^+$ / $CD45^+$ cells, $F4/80^+$ / $CD11b^+$ cells, $CD86^+$ / $F4/80^+$ cells and $CD163^+$ / $F4/80^+$ cells in tumors were determined by flow cytometry. Data with error bars are shown as mean ± SEM. ns, not significant; *P < 0.05, **P < 0.01, ***P < 0.001, ****P < 0.0001.

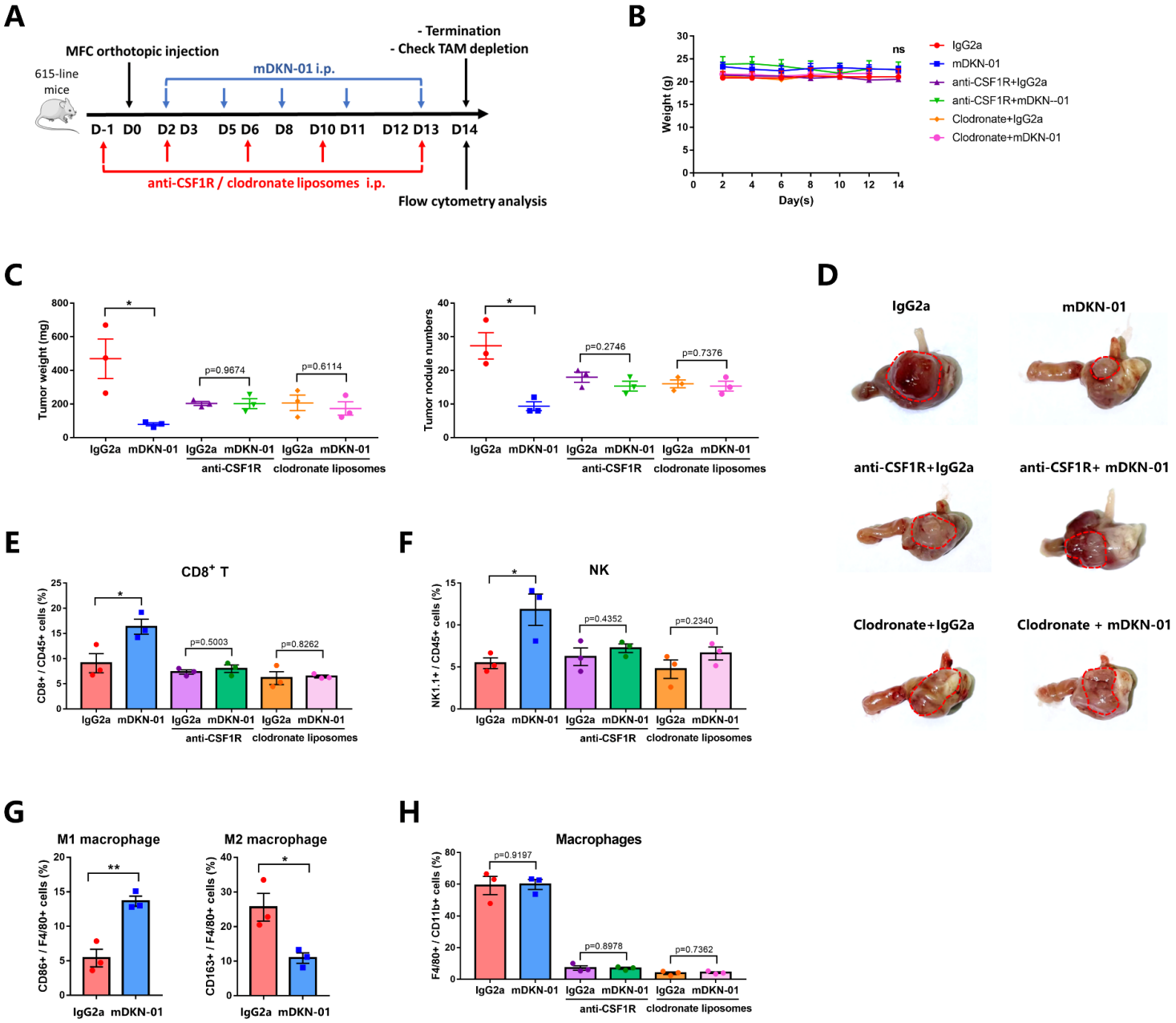

Fig. S13. DKK1 blockade fails to trigger anti-tumor effect or improve the TIME of orthotopic GC model with TAM depletion. (A) Schematic of TAM depletion by clodronate liposomes or anti-CSF1R, and mDKN-01 treatment in orthotopic GC model. **(B)** Body weight, **(C)** orthotopic tumor weight and numbers of metastatic tumor nodules in the abdominal cavity of 615-line mice treated with clodronate liposomes, anti-CSF1R, mDKN-01 or IgG2a (n=3 per group). **(D)** Mice were sacrificed on day 14 and the stomachs were removed for analysis. **(E)** The proportions of $CD8^+$ / $CD45^+$ cells, **(F)** $NK1.1^+$ / $CD45^+$ cells, **(G)** $CD86^+$ / $F4/80^+$ cells, $CD163^+$ / $F4/80^+$ cells and **(H)**

F4/80$^+$ / CD11b$^+$ cells in the orthotopic tumors were determined by flow cytometry. Data with error bars are shown as mean ± SEM. ns, not significant; *P < 0.05, **P < 0.01, ***P < 0.001, ****P < 0.0001.

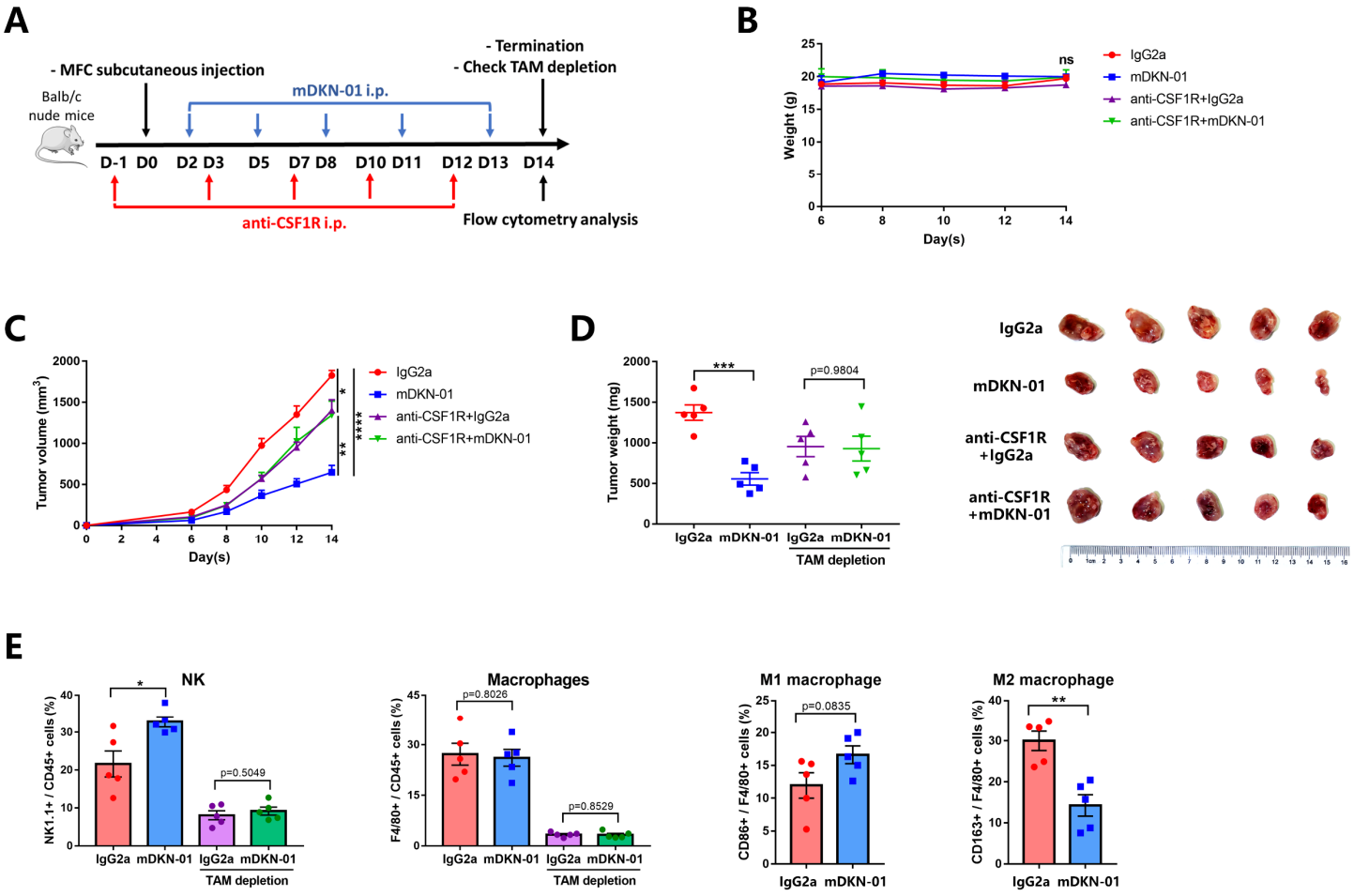

Fig. S14. DKK1 blockade fails to trigger anti-tumor effects or improve the TIME of T cell-deficient GC model with TAM depletion. (A) Schematic of TAM depletion by anti-CSF1R, and mDKN-01 treatment in T cell-deficient GC model. **(B)** Body weight, **(C)** tumor volume and (D) tumor weight of Balb/c nude mice treated with anti-CSF1R, mDKN-01 or IgG2a (n=5 per group). Mice were sacrificed on day 14 and the tumors were removed for analysis. **(E)** The proportions of NK1.1$^+$ / CD45$^+$ cells, F4/80$^+$ / CD45$^+$ cells, CD86$^+$ / F4/80$^+$ cells and CD163$^+$ / F4/80$^+$ cells in the tumors were determined by flow cytometry. Data with error bars are shown as mean ± SEM. ns, not significant; *P < 0.05, **P < 0.01, ***P < 0.001, ****P < 0.0001.

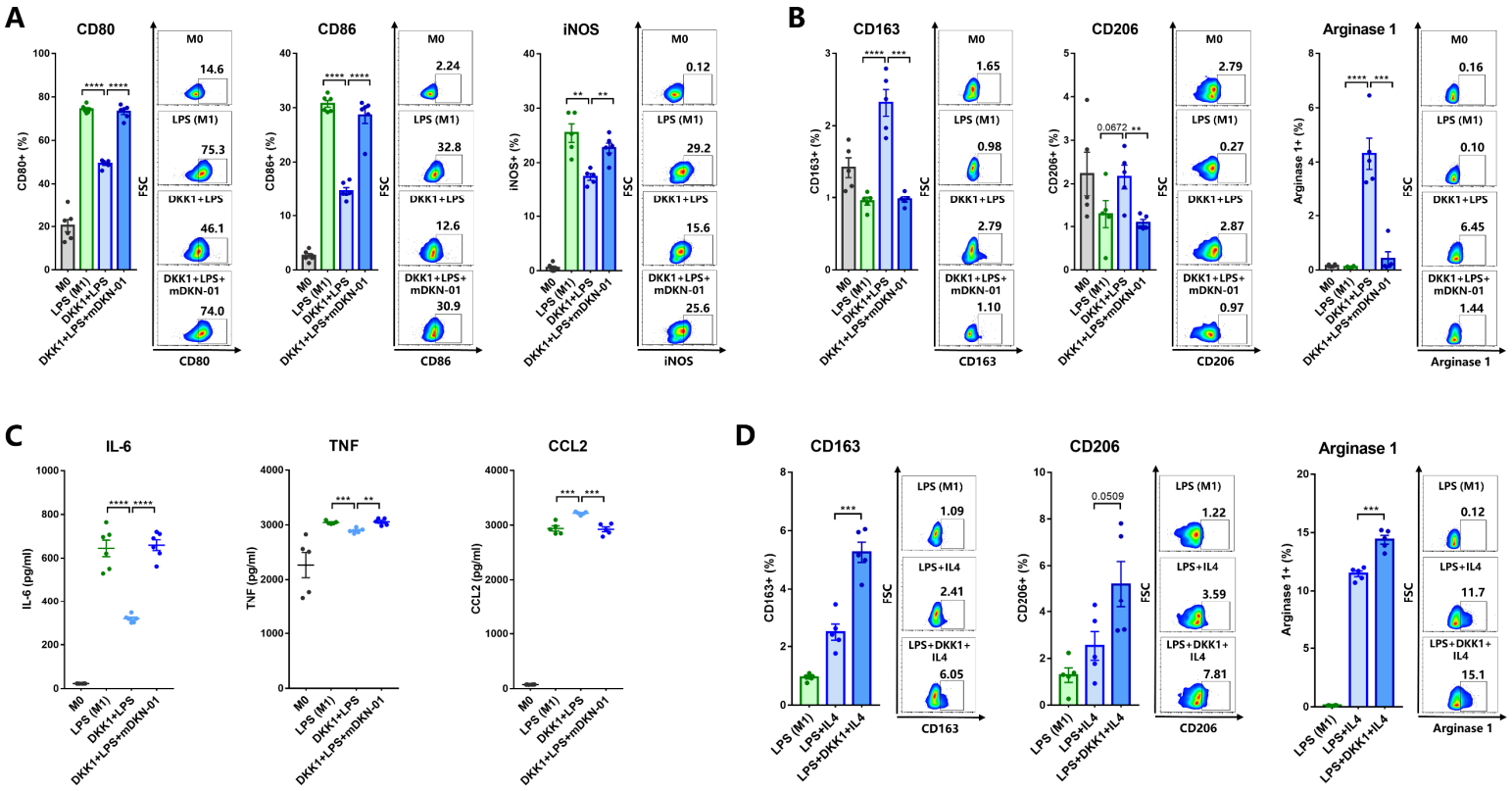

Fig. S15. DKK1 induces immune suppression in RAW264.7 cells. RAW264.7 were pretreated for 5h with recombinant DKK1 protein (50 ng/ml), followed by LPS (50 ng/ml) stimulation with or without mDKN-01 (50 μg/ml) administration. After 48h culture, the proportions of **(A)** $CD80^+$, $CD86^+$, $iNOS^+$ cells, **(B)** $CD163^+$, $CD206^+$ and Arginase 1^+ cells were determined by flow cytometry. **(C)** Concentrations of IL-6, TNF and CCL2 were detected by CBA in cell supernatants of RAW264.7. To induce the M1 to M2 phenotype transition, RAW264.7 cells were pretreated for 5h with LPS (50 ng/ml), followed by IL4 (20 ng/ml) administration or DKK1 (50 ng/ml) and IL4 (20 ng/ml) co-administration. After 48h culture, the proportions of **(D)** $CD163^+$, $CD206^+$ and Arginase 1^+ cells were determined by flow cytometry. Each group contains at least five independent biological replicates. Data with error bars are shown as mean ± SEM. ns, not significant; $*P < 0.05$, $**P < 0.01$, $***P < 0.001$, $****P < 0.0001$.

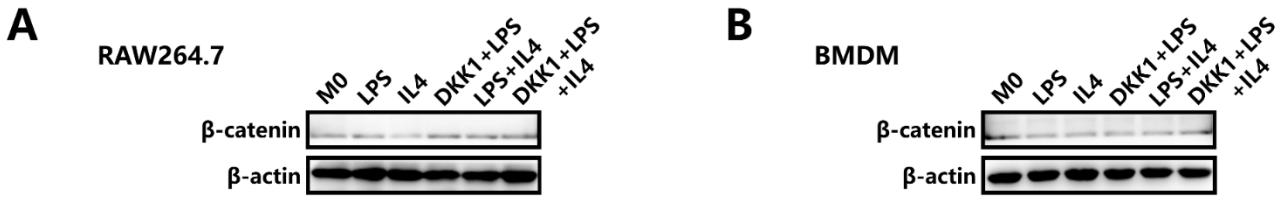

Fig. S16. β-catenin expression of murine macrophages from different treatment groups. Western blot analysis of β-catenin and β-actin in **(A)** RAW264.7 and **(B)** 615-line mice derived BMDM administrated with or without DKK1 (50 ng/ml), LPS (50 ng/ml) and IL4 (20 ng/ml).

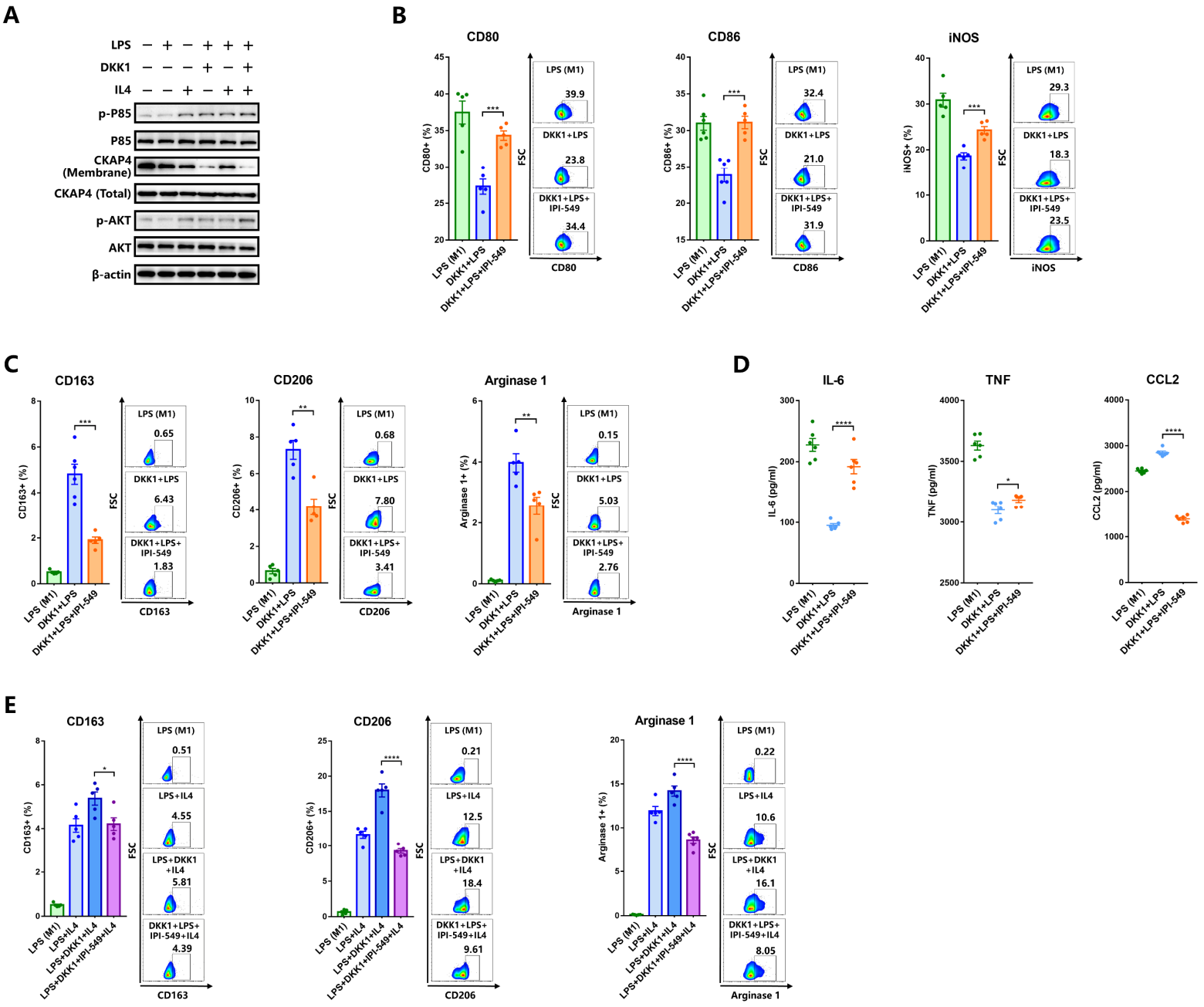

Fig. S17. DKK1 induces immune suppression in RAW264.7 cells. (A) Western blot analysis of p-P85, P85, membrane CKAP4, total CKAP4, p-Akt, Akt and β-actin in RAW264.7 administrated with or without DKK1 (50 ng/ml), LPS (50 ng/ml) and IL4 (20 ng/ml). For analysis of PI3K-AKT signaling, RAW264.7 cells were additionally treated with IPI-549 (PI3Kγ inhibitor, 1 μM) in the co-culture assay described above, and the proportions of **(B)** $CD80^+$, $CD86^+$, $iNOS^+$ cells, **(C)** $CD163^+$, $CD206^+$ and Arginase 1^+ cells were determined by flow cytometry. **(D)** Concentrations of IL-6, TNF and CCL2 were detected by CBA in cell supernatants of RAW264.7. In M1 to M2 phenotype transition process, RAW264.7 cells were additionally treated with IPI-549 (1 μM), and

the proportions of **(E)** $CD163^+$, $CD206^+$ and Arginase 1^+ cells were determined by flow cytometry. Each group contains at least five independent biological replicates. Data with error bars are shown as mean ± SEM. ns, not significant; *$P < 0.05$, **$P < 0.01$, ***$P < 0.001$, ****$P < 0.0001$.

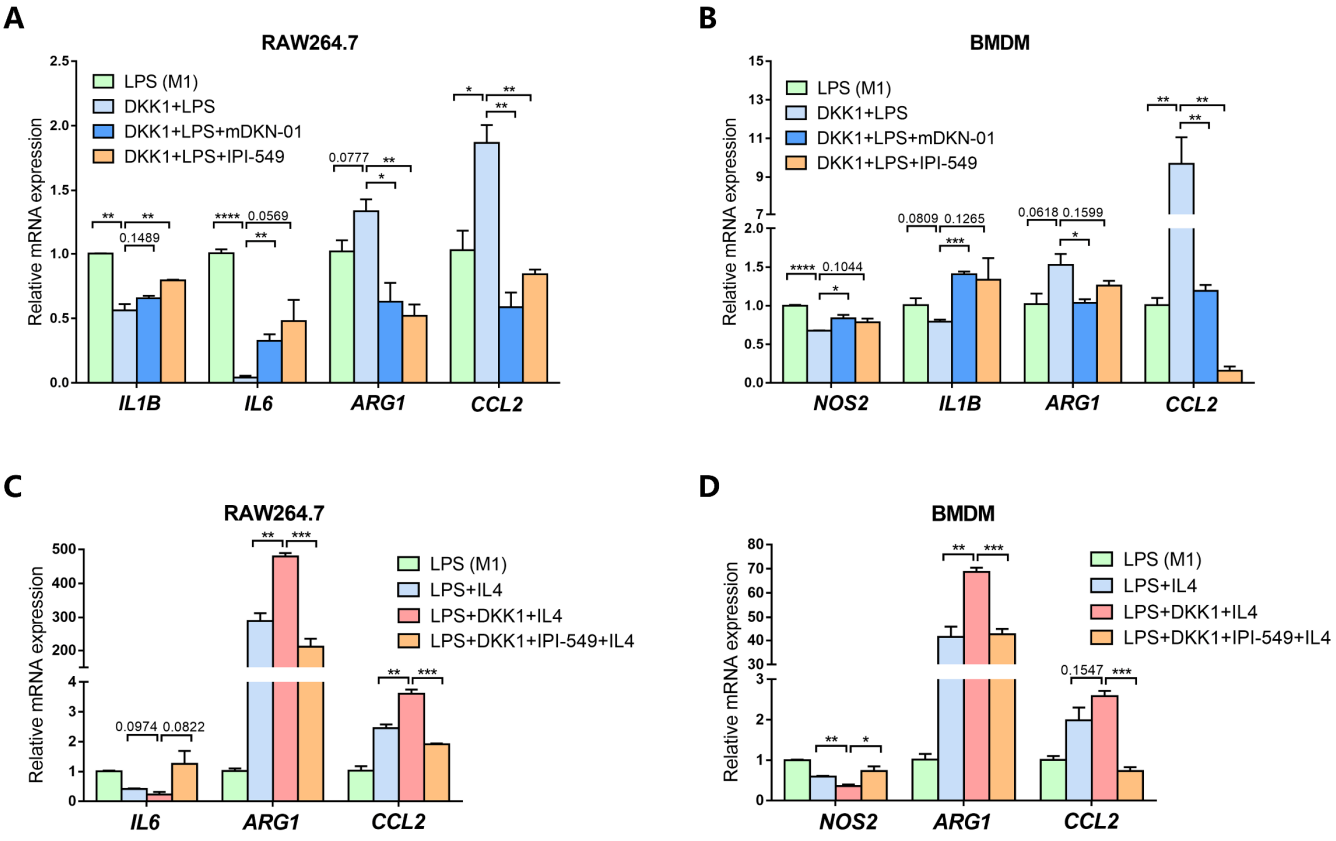

Fig. S18. The immunosuppressive suppression in macrophages mediated by DKK1-PI3K-AKT signaling is confirmed at mRNA level. (A) RAW264.7 and **(B)** 615-line BMDMs were pretreated for 5h with recombinant DKK1 protein (50 ng/ml), followed by LPS (50 ng/ml) stimulation with or without mDKN-01 (10 μg/ml) or IPI-549 (1 μM) administration. After 48h culture, the mRNA expressions of *NOS2*, *IL1B*, *IL6*, *ARG1*, *CCL2* were detected by RT-qPCR. To induce M1 to M2 phenotype transition, **(C)** RAW264.7 and **(D)** 615-line BMDMs were pretreated for 5h with LPS (50 ng/ml), followed by IL4 (20 ng/ml) administration or DKK1 (50 ng/ml) + IL4 (20 ng/ml) or DKK1 (50 ng/ml) + IPI-549 (1 μM) + IL4 (20 ng/ml) co-administration. After 48h culture, the mRNA expressions of *NOS2*, *IL6*, *ARG1*, *CCL2* were detected by RT-qPCR. Each group contains three independent biological replicates. Data with error bars are shown as mean ± SEM. ns, not significant; **P* < 0.05, ***P* < 0.01, ****P* < 0.001, *****P* < 0.0001.

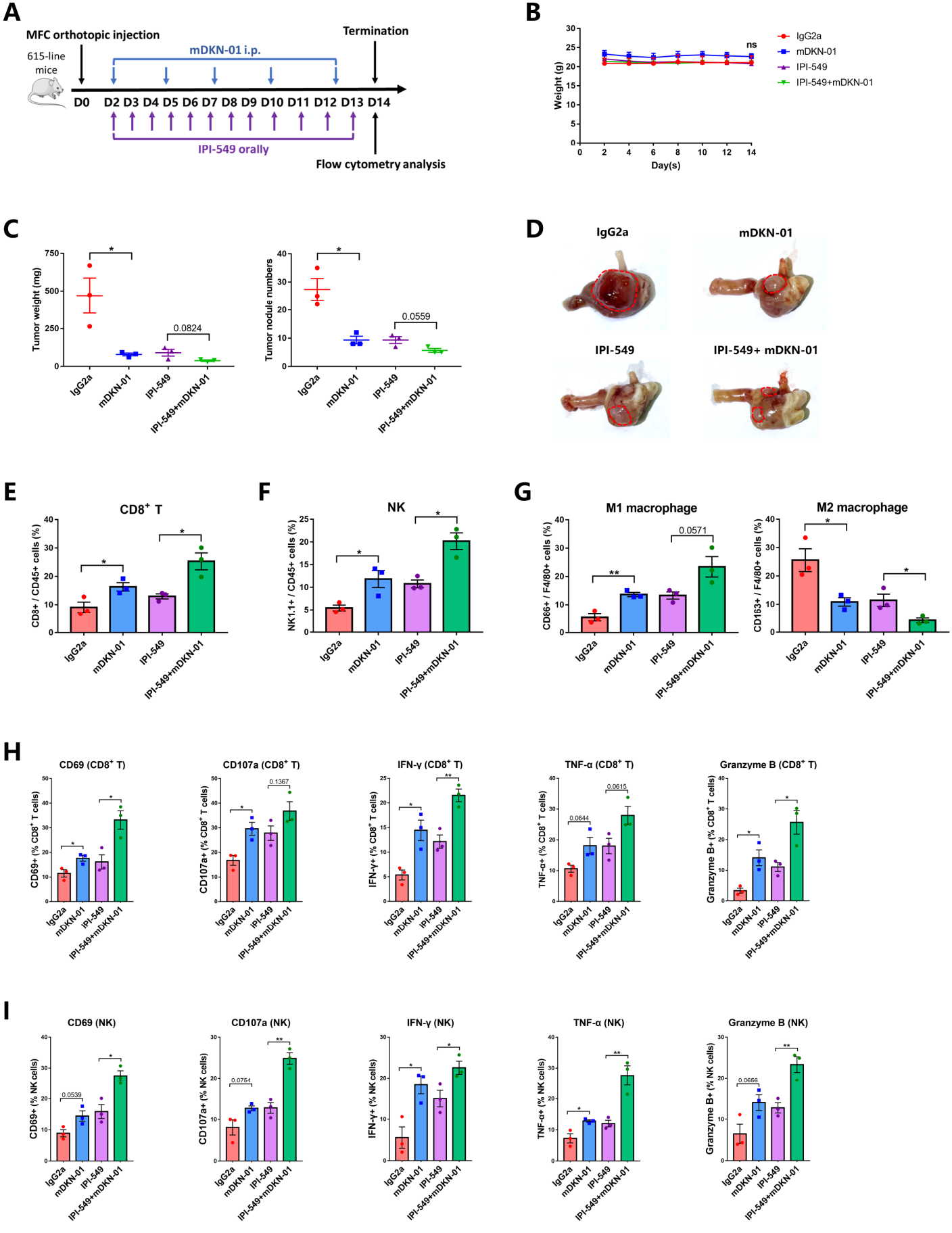
A
MFC orthotopic injection
615-line mice
mDKN-01 i.p.
Termination
D0 D2 D3 D4 D5 D6 D7 D8 D9 D10 D11 D12 D13 D14
IPI-549 orally
Flow cytometry analysis
B
Weight (g)
Day(s)
ns
IgG2a
mDKN-01
IPI-549
IPI-549+mDKN-01
C
Tumor weight (mg)
Tumor nodule numbers
0.0824
0.0559
D
IgG2a
mDKN-01
IPI-549
IPI-549+ mDKN-01
E
CD8+ T
CD3+ / CD45+ cells (%)
F
NK
NK1.1+ / CD45+ cells (%)
G
M1 macrophage
CD86+ / F4/80+ cells (%)
0.0571
M2 macrophage
CD163+ / F4/80+ cells (%)
H
CD69 (CD8+ T)
CD69+ (% CD8+ T cells)
CD107a (CD8+ T)
CD107a+ (% CD8+ T cells)
0.1367
IFN-γ (CD8+ T)
IFN-γ+ (% CD8+ T cells)
TNF-α (CD8+ T)
TNF-α+ (% CD8+ T cells)
0.0644
0.0615
Granzyme B (CD8+ T)
Granzyme B+ (% CD8+ T cells)
I
CD69 (NK)
CD69+ (% NK cells)
0.0539
CD107a (NK)
CD107a+ (% NK cells)
0.0764
IFN-γ (NK)
IFN-γ+ (% NK cells)
TNF-α (NK)
TNF-α+ (% NK cells)
Granzyme B (NK)
Granzyme B+ (% NK cells)
0.0666

Fig. S19. Targeting DKK1-PI3K-AKT signaling reprograms macrophages and activates cytotoxic lymphocytes in the orthotopic GC model. (A) Schematic of mDKN-01, IgG2a or IPI-549 treatment in orthotopic GC model. **(B)** Body weight, **(C)** orthotopic tumor weight and numbers of metastatic tumor nodules in the abdominal cavity of 615-line mice treated with mDKN-01, IPI-549 or IgG2a (n=3 per group). **(D)** Mice were sacrificed on day 14 and the stomachs were removed for analysis. The proportions of **(E)** $CD8^+$ / $CD45^+$ cells, **(F)** $NK1.1^+$ / $CD45^+$ cells, **(G)** $CD86^+$ / $F4/80^+$ cells, $CD163^+$ / $F4/80^+$ cells in the orthotopic tumors were determined by flow cytometry. The activations of **(H)** $CD8^+$ T cells and **(I)** NK cells were measured by expression of CD69, CD107a, IFN-γ, TNF-α and Granzyme B by flow cytometry. Data with error bars are shown as mean ± SEM. ns, not significant; *P < 0.05, **P < 0.01, ***P < 0.001, ****P < 0.0001.

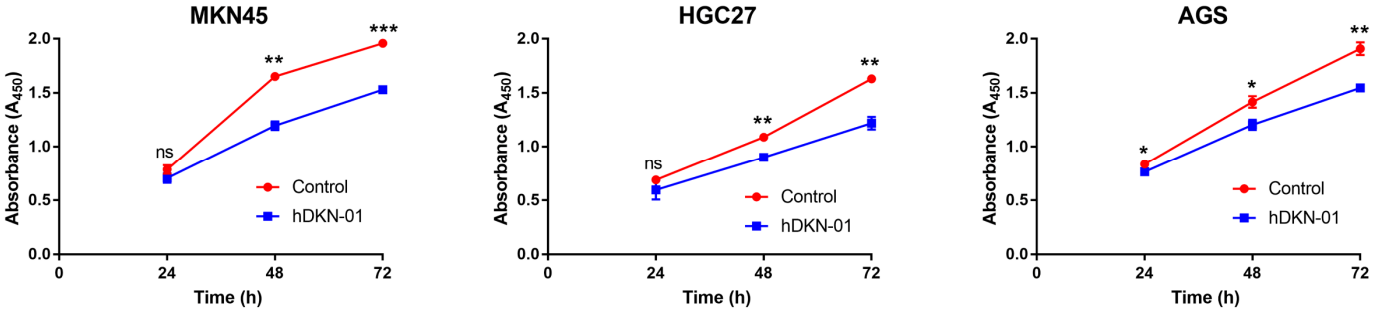

Fig. S20. Effects of DKK1 blockade on human GC cell lines with high DKK1 expression. Human GC cell lines with high DKK1 expression (MKN45, HGC27 and AGS) were seeded in 96-well plates at 4000 cells per well and treated with mDKN-01 at 10 μg/ml. After 24h, 48h or 72h co-culture, cell viability was measured by CCK-8 assay. Each experiment contains three independent biological replicates. Data with error bars are shown as mean ± SEM. ns, not significant; *$P < 0.05$, **$P < 0.01$, ***$P < 0.001$, ****$P < 0.0001$.

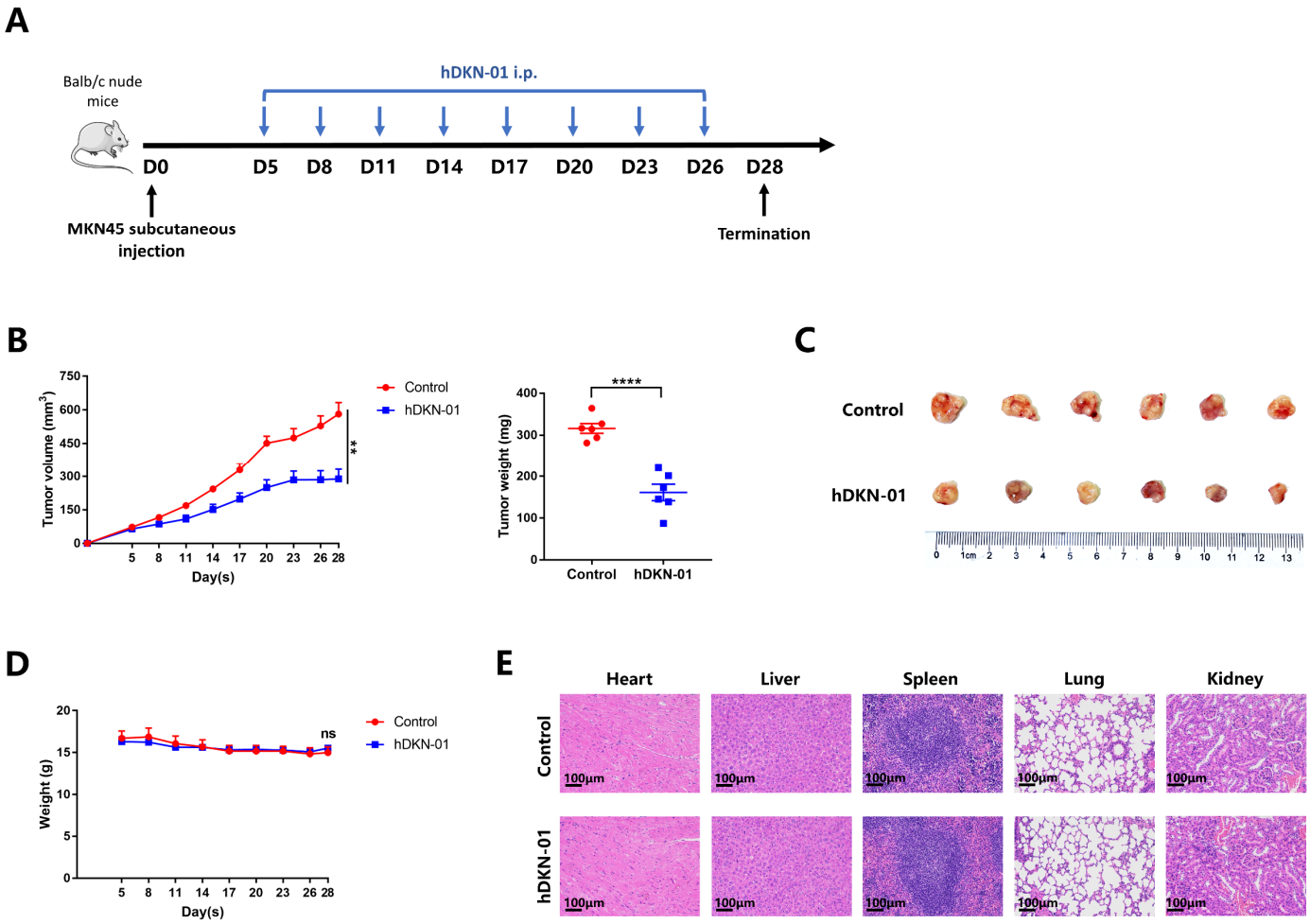

Fig. S21. DKK1 blockade triggers anti-tumor effects in xenograft GC model. (A) Schematic of mDKN-01 treatment schedule in xenograft GC model. Balb/c nude mice (n=6 per group) were injected s.c. with $5*10^6$ MKN45 cells and treated i.p. with hDKN-01 (10 mg/kg) eight times in 28 days. **(B)** Tumor volumes and tumor weight of mice in xenograft GC model. **(C)** Mice were sacrificed on day 28 and tumors were removed for analysis. **(D)** Body weight of mice in xenograft GC model. **(E)** Hematoxylin and eosin (H&E) staining of mouse organs (heart, liver, spleen, lung and kidney) from xenograft GC model is shown (Scale bars, 100 μm). Data with error bars are shown as mean ± SEM. *$P < 0.05$, **$P < 0.01$, ***$P < 0.001$, ****$P < 0.0001$.